



This is a repository copy of *Mucoromycotina fine root endophyte fungi form nutritional mutualisms with vascular plants*.

White Rose Research Online URL for this paper:
<http://eprints.whiterose.ac.uk/163879/>

Version: Accepted Version

Article:

Hoysted, G.A., Jacob, A.S., Kowal, J. et al. (8 more authors) (2019) *Mucoromycotina fine root endophyte fungi form nutritional mutualisms with vascular plants*. *Plant Physiology*, 181 (2). pp. 565-577. ISSN 0032-0889

<https://doi.org/10.1104/pp.19.00729>

© 2019 The Author(s). This is an author-produced version of a paper subsequently published in *Plant Physiology*. Uploaded in accordance with the publisher's self-archiving policy.

Reuse

Items deposited in White Rose Research Online are protected by copyright, with all rights reserved unless indicated otherwise. They may be downloaded and/or printed for private study, or other acts as permitted by national copyright laws. The publisher or other rights holders may allow further reproduction and re-use of the full text version. This is indicated by the licence information on the White Rose Research Online record for the item.

Takedown

If you consider content in White Rose Research Online to be in breach of UK law, please notify us by emailing eprints@whiterose.ac.uk including the URL of the record and the reason for the withdrawal request.



eprints@whiterose.ac.uk
<https://eprints.whiterose.ac.uk/>

1 **Mucoromycotina fine root endophyte fungi form nutritional mutualisms with vascular**
2 **plants.**

3

4 Grace A. Hoysted¹, Alison S. Jacob^{2,3}, Jill Kowal⁴, Philipp Giesemann⁵, Martin I.

5 Bidartondo^{2,3}, Jeffrey G. Duckett⁴, Gerhard Gebauer⁵, William R. Rimington^{2,3,4}, Sebastian

6 Schornack⁶, Silvia Pressel⁴ and Katie J. Field^{1*}

7

8 ¹ Centre for Plant Sciences, Faculty of Biological Sciences, University of Leeds, Leeds, LS2

9 9JT, UK

10 ² Comparative Plant & Fungal Biology, Royal Botanic Gardens, Kew, Richmond TW9 3DS,

11 UK

12 ³ Department of Life Sciences, Imperial College London, London, SW7 2AZ, UK

13 ⁴ Department of Life Sciences, Natural History Museum, London SW7 5BD, UK

14 ⁵ Laboratory of Isotope Biogeochemistry, Bayreuth Center of Ecology and Environmental
15 Research (BayCEER), University of Bayreuth, Bayreuth, Germany

16 ⁶ Sainsbury Laboratory, University of Cambridge, Cambridge, CB2 1LR

17

18 *Corresponding author:

19 Katie J. Field (k.field@leeds.ac.uk)

20 Tel: +44 (0)113 343 2849

21

22 **Competing interests statement**

23 The authors declare no competing financial interests.

24

25

26 **Abstract**

27 Fungi and plants have engaged in intimate symbioses that are globally widespread and have
28 driven terrestrial biogeochemical processes since plant terrestrialisation >500 Mya. Recently,

29 hitherto unknown nutritional mutualisms involving ancient lineages of fungi and non-vascular
30 plants have been discovered. However, their extent and functional significance in vascular
31 plants remains uncertain. Here, we provide first evidence of abundant carbon-for-nitrogen
32 exchange between an early-diverging vascular plant (Lycopodiaceae) and Mucoromycotina
33 (Endogonales) fine root endophyte regardless of changes in atmospheric CO₂ concentration.
34 Furthermore, we provide evidence that the same fungi also colonize neighbouring non-
35 vascular and flowering plants. These findings fundamentally change our understanding of
36 the evolution, physiology, interrelationships and ecology of underground plant-fungal
37 symbioses in terrestrial ecosystems by revealing an unprecedented nutritional role of
38 Mucoromycotina fungal symbionts in vascular plants.

39

40 **Key Words**

41 *Arbuscular mycorrhizas, Endogonales, fine root endophyte (FRE), lycophytes,*
42 *Mucoromycotina, mutualism, nitrogen, carbon, plant-fungus symbiosis, vascular plants.*

43

44 **Introduction**

45 Plant terrestrialisation >500 Mya [1] was facilitated by the formation of mutualistic symbioses
46 with fungi, through which the earliest plants gained access to mineral nutrients in exchange
47 for photosynthetically-fixed carbon (C) under ancient, high atmospheric CO₂ concentrations
48 (a[CO₂]) [2]. It was long hypothesised that this ancient mycorrhizal-like symbiosis was
49 closely related to and subsequently evolved into widespread modern-day arbuscular
50 mycorrhizas (AM) formed with plant roots by Glomeromycotina fungi [3, 4]. However, recent
51 molecular, cytological, physiological and paleobotanical evidence has strongly indicated that
52 early fungal associates were likely to be more diverse than has previously been assumed [5-
53 7]. Members of the earliest diverging clade of an ancient land plant lineage, Haplomitriopsida
54 liverworts, are now known to form a[CO₂]-responsive mycorrhizal-like associations with
55 Mucoromycotina fungi [5, 8] which also colonise other early diverging plant lineages, namely
56 hornworts, lycophytes and ferns [9, 10]. Mucoromycotina represent an ancient fungal lineage

57 considered to branch earlier than, or sister to, the Glomeromycotina [11, 12], thus its recent
58 identification in a range of modern non-vascular plants [6] and plant fossils [7, 13] supports
59 the idea that the colonisation of Earth's land masses by plants was facilitated not only by
60 Glomeromycotina but also by Mucoromycotina fungal symbionts [14]. Latest discoveries of
61 putative Mucoromycotina fungi in vascular land plants [10, 15, 16] indicate that root
62 symbiotic versatility and diversity [17] has been grossly underestimated across extant plants.

63 Although Mucoromycotina fungal symbioses in non-vascular plants have, to date,
64 received most attention [5, 6, 9, 18], there are now several reports of their occurrence in
65 vascular plants [10, 15-17, 19]. It has been suggested that the globally widespread,
66 arbuscule-forming fine root endophytes (FRE), classified as *Glomus tenue* (or
67 *Planticonsortium tenue* [20]), and which occur across a wide range of vascular groups [19]
68 are closely related to the Mucoromycotina symbionts of non-vascular plants. These findings
69 have major ramifications for our understanding of the past and present diversity and function
70 of plant-fungal nutritional symbioses [21], suggesting Mucoromycotina fungal symbiosis is
71 not limited to ancient plant lineages but is in fact widespread throughout extant land plants.
72 However, it remains unclear whether the putative Mucoromycotina FRE fungi detected in
73 vascular plants to date are the same in terms of function and identity as the mutualistic
74 Mucoromycotina fungal symbionts detected in non-vascular plants.

75 As lycophytes are considered to be the earliest divergent extant vascular plant
76 lineage [22], the discovery of non-Glomeromycotina fungal associates in lycophyte roots and
77 gametophytes is particularly significant. For over 100 years, the fungal associations in
78 lycophytes have been thought of as being AM-like but with unique "lycopodioid" features [23].
79 However, global analysis of fungal associates in 20 lycophytes [15] has now shown their
80 colonisation is broadly similar to that of hornworts [9], with many species forming single
81 and/or dual associations with both Glomeromycotina arbuscular mycorrhiza fungi (AMF) and
82 Mucoromycotina FRE fungi [15]. Remarkably, every sample of *Lycopodiella inundata* - a
83 species common in wet habitats across the Northern Hemisphere - examined so far appears

84 colonised exclusively by Mucoromycotina FRE fungi [15]. Since a major obstacle to studying
85 Mucoromycotina FRE function has been finding plants that are not co-colonized by coarse
86 root endophytes (i.e. Glomeromycotina AMF) [19], *L. inundata* provides a unique and
87 important opportunity to dissect the symbiotic function of FRE in a vascular plant. This is
88 particularly pertinent given that the functional significance of Mucoromycotina FRE
89 associations in vascular plants and their response to changing a[CO₂] relevant to conditions
90 during the Paleozoic era and the time of vascular plant divergence are completely unknown
91 [17, 19]. Indeed, there is no evidence of nutritional mutualism between any vascular plant
92 and Mucoromycotina FRE [17].

93 Here, we address these critical knowledge gaps by investigating the cytology,
94 function and identity of the fungal association in *L. inundata* (Figure 1 a, b) under simulated
95 ancient and modern a[CO₂]. We use a combination of molecular biology, radio- and stable
96 isotope tracers, and cytological analyses to address the following questions:

- 97 (1) Do Mucoromycotina fungal symbionts of *L. inundata* co-occur in neighbouring
98 angiosperm roots and non-vascular plant rhizoids?
- 99 (2) Are there characteristic cytological signatures or features of Mucoromycotina
100 fungal associations in *L. inundata* compared to those formed in non-vascular
101 plants?
- 102 (3) What is the function of Mucoromycotina fungal associations in lycophytes in
103 terms of carbon-for-nutrient exchange and is it affected by a[CO₂]?

104

105

106 **Methods**

107 *Plant material*

108 *Lycopodiella inundata* (L.), neighbouring angiosperms (the grasses *Holcus lanatus*,
109 *Molinia caerulea* and the rush *Juncus bulbosus*), and liverworts (*Fossombronia foveolata*)
110 were collected from Thursley National Nature Reserve, Surrey, UK (SU 90081 39754) in
111 June 2017. The *L. inundata* plants were planted directly into pots (90 mm diameter x 85 mm
112 depth) containing acid-washed silica sand. Soil surrounding plant roots was left intact and
113 pots were weeded regularly to remove other plant species. The other plants collected in
114 Thursley, and additional plants from three other UK field sites (Supplementary Table S1),
115 were used for cytological and molecular analyses. Additional vascular plants from Thursley
116 were used for stable isotope analyses.

117 *Growth conditions*

118 Based on the methods of Field *et al.* [8], three windowed cylindrical plastic cores
119 covered in 10 µm nylon mesh (Supplementary Figure S1) were inserted into the substrate
120 within each experimental pot. Two of the cores were filled with a homogenous mixture of
121 acid-washed silica sand, compost (Petersfield No.2, Leicester, UK) and native soil gathered
122 from around the roots of wild plants (in equal parts making up 99% of the core volume) and
123 fine-ground tertiary basalt (1% core volume) [8]. The third core was filled with glass wool to
124 allow below-ground gas sampling throughout the ¹⁴C-labelling period to monitor soil
125 community respiration.

126 The *L. inundata* plants were maintained in controlled environment chambers (Micro
127 Clima 1200, Snijders Labs, The Netherlands). Plants were grown at two contrasting CO₂
128 atmospheres; 440 ppm a[CO₂] to represent a modern-day atmosphere, or at 800 ppm
129 a[CO₂] to simulate Paleozoic atmospheric conditions on Earth at the time vascular plants are
130 thought to have diverged [2]. a[CO₂] was monitored using a Vaisala sensor system (Vaisala,
131 Birmingham, UK), maintained through addition of gaseous CO₂. Cabinet settings and
132 contents were alternated every four weeks, and all pots were rotated within cabinets to
133 control for cabinet and block effects. Plants were acclimated to chamber/growth regimes

134 (see Supplementary Information) for four weeks to allow establishment of mycelial networks
135 within pots and confirmed by hyphal extraction from soil and staining with trypan blue [24].
136 Additionally, roots were stained with acidified ink for the presence of fungi, based on the
137 methods of Brundrett *et al.* [24].

138 *Molecular identification of fungal symbionts*

139 All plants (Supplementary Table S1) were processed for molecular analyses within
140 one week of collection. Genomic DNA extraction and purification from all specimens and
141 subsequent amplification, cloning and sequencing were performed according to methods
142 from Rimington *et al.* [10]. The fungal 18S ribosomal rRNA gene was targeted using the
143 broad specificity fungal primer set NS1/EF3 and a semi-nested approach with
144 Mucoromycotina- and Glomeromycotina-specific primers described in Desirò *et al.* [9] for the
145 experimental *L. inundata* plants and all other field collected plant material using
146 Mucoromycotina-specific primers. Resulting partial 18S rDNA sequences were edited and
147 preliminarily identified with BLAST in Geneious v. 8.1.7 [25]. Chimeric sequences were
148 detected using the UCHIME2 algorithm [26] in conjunction with the most recent non-
149 redundant SSU SILVA database (SSU Ref NR 132, December 2017, www.arb-silva.de).
150 Sequences identified as Mucoromycotina sp. were aligned with MAFFT prior to removing
151 unreliable columns using the default settings in GUIDANCE2 (<http://guidance.tau.ac.il>). The
152 best-fit nucleotide model for phylogenetic analysis was calculated using Smart Model
153 Selection [27]. Maximum Likelihood (ML) with 1,000 replicates was performed using PhyML
154 3.0 [28]. Bayesian inference analysis was conducted in Mr Bayes version 3.2.6 [29] with four
155 Markov chain Monte Carlo (MCMC) strands and 10^6 generations. Consensus trees were
156 produced after excluding an initial burn-in of 25% of the samples (Supplementary Figures
157 S2-8). Representative DNA sequences were deposited in GenBank.

158 *Cytological analyses*

159 *Lycopodiella inundata* gametophytes, young sporophytes (protocorms) and roots of
160 mature plants (both wild and experimental), roots of angiosperms (*Holcus lanatus*, *Molinia*

161 *caerulea* and *Juncus bulbosus*), and liverwort gametophytes (*Fossombronia foveolata*) were
162 either stained with trypan blue [24], which is common standard for identifying FRE [19], and
163 photographed under a Zeiss Axioscope (Zeiss, Oberkochen, Germany) equipped with a
164 MRc digital camera, or processed for scanning electron microscopy (SEM) within 48 hrs of
165 collection [30]. For SEM we followed the protocol by Duckett *et al.* [31] (see Supplementary
166 Information). For experimental plants of *L. inundata*, ten randomly selected roots per
167 treatment were cut into up to six segments (depending on root length) and colonization by
168 FRE scored as absent or present for each segment under the SEM.

169 *Quantification of C, ³³P and ¹⁵N fluxes between lycophytes and fungi*

170 After the four-week acclimation period, 100 µl of an aqueous mixture of ³³P-labelled
171 orthophosphate (specific activity 111 TBq mmol⁻¹, 0.3 ng ³³P added; Hartmann analytics,
172 Braunschweig, Germany) and ¹⁵N-ammonium chloride (1mg ml⁻¹; 0.1 mg ¹⁵N added; Sigma,
173 Dorset, UK) was introduced into one of the soil-filled mesh cores in each pot through the
174 installed capillary tube (Supplementary Figure S9a). In half (12) of the pots, cores containing
175 isotope tracers were left static to preserve direct hyphal connections with the lycophytes.
176 Fungal access to isotope tracers was limited in the remaining half (12) of the pots by rotating
177 isotope tracer-containing cores through 90°, thereby severing the hyphal connections
178 between the plants and core soil. These were rotated every second day thereafter, thus
179 providing a control treatment that allows us to distinguish between fungal and microbial
180 contributions to tracer uptake by plants. Assimilation of ³³P tracer into above-ground plant
181 material was monitored using a hand-held Geiger counter held over the plant material daily.

182 At detection of peak activity in above-ground plant tissues (21 days after the addition
183 of the ³³P and ¹⁵N tracers), the tops of ³³P and ¹⁵N-labelled cores were sealed with plastic
184 caps and anhydrous lanolin and the glass wool cores were sealed with rubber septa
185 (SubaSeal, Sigma, Dorset, UK). Each pot was sealed into a 3.5 L, gas-tight labelling
186 chamber and 2 ml 10% lactic acid was added to 30 µl NaH¹⁴CO₃ (specific activity 1.621

187 GBq/mmol⁻¹; Hartmann Analytics, Braunschweig, Germany) in a cuvette within the chamber
188 prior to cabinet illumination at 0800 (Supplementary Figure S9b), releasing a 1.1-MBq pulse
189 of ¹⁴CO₂ gas. Pots were maintained under growth chamber conditions, and 1 ml of gas was
190 sampled after 1 hour and every 1.5 hours thereafter. Below-ground respiration was
191 monitored via gas sampling from within the glass-wool filled core after 1 hour and every 1.5
192 hours thereafter for ~16 h.

193 *Plant harvest and sample analyses*

194 Upon detection of maximum below-ground flux of ¹⁴C, plant materials and soil were
195 separated, freeze-dried, weighed and homogenised. The ³³P activity in plant and soil
196 samples was quantified by digesting in concentrated H₂SO₄ (see Supplementary
197 Information) and liquid scintillation (Tricarb 3100TR liquid scintillation analyser, Isotech,
198 Chesterfield, UK). The quantity of ³³P tracer that was transferred to the plant by its fungal
199 partner was then calculated using previously published equations [32] (see Supplementary
200 Information). Total ³³P in plants without access to the tracer through core rotation (i.e.
201 assimilated through alternative soil microbial P-cycling processes and/or diffusion from core)
202 was subtracted from the total ³³P in plants with access to the core contents via intact fungal
203 hyphal connections to give fungal acquired ³³P.

204 Between two and four mg of freeze-dried, homogenised plant tissue was weighed
205 into 6 x 4 mm² tin capsules (Sercon Ltd. Irvine, UK) and ¹⁵N abundance was determined
206 using a continuous flow IRMS (PDZ 2020 IRMS, Sercon Ltd. Irvine, UK). Air was used as
207 the reference standard, and the IRMS detector was regularly calibrated to commercially
208 available reference gases. The ¹⁵N transferred from fungus to plant was then calculated
209 using equations published previously [18] (see Supplementary Information). Total ¹⁵N in
210 plants without access to the isotope because of broken hyphal connections between plant
211 and core contents was subtracted from total ¹⁵N in plants with intact hyphal connections to
212 the mesh-covered core to give fungal-acquired ¹⁵N.

213 The ^{14}C activity of plant and soil samples was quantified through sample oxidation
214 (307 Packard Sample Oxidiser, Isotech, Chesterfield, UK) followed by liquid scintillation.
215 Total C ($^{12}\text{C} + ^{14}\text{C}$) fixed by the plant and transferred to the fungal network was calculated as
216 a function of the total volume and CO_2 content of the labelling chamber and the proportion of
217 the supplied $^{14}\text{CO}_2$ label fixed by plants (see Supplementary Information). The difference in
218 total C between the values obtained for static and rotated core contents is considered
219 equivalent to the total C transferred from plant to symbiotic fungus within the soil core, noting
220 that a small proportion will be lost through soil microbial respiration. The total C budget for
221 each experimental pot was calculated using equations from Cameron *et al.* [33] (see
222 Supplementary Information).

223 *Stable isotope signatures of neighbouring plants*

224 *Lycopodiella inundata* and *J. bulbosus* were collected from Thursley National Nature
225 Reserve, Surrey, together with co-occurring reference plants from six 1 m² plots in May 2018,
226 following the sampling scheme of Gebauer and Meyer [34]. Five plant species representing
227 three different types of mycorrhizal associations served as reference plants: two ericoid
228 mycorrhizal species (*Erica tetralix*, collected on six plots; *Calluna vulgaris*, collected on three
229 plots), two ectomycorrhizal species (*Pinus sylvestris* and *Betula pendula* seedlings, both
230 from one plot) and one arbuscular mycorrhizal species (*Molinia caerulea* from six plots).
231 Relative C and N isotope natural abundances of dried and ground leaf and root samples
232 were measured in a dual element analysis mode with an elemental analyser (Carlo Erba
233 Instruments 1108, Milan, Italy) coupled to a continuous flow isotope ratio mass spectrometer
234 (delta S, Finnigan MAT, Bremen, Germany) via a ConFlo III open-split interface (Thermo
235 Fisher Scientific, Bremen, Germany) as described in Bidartondo *et al.* [35]. Relative isotope
236 abundances (δ values) were calculated, calibrated and checked for accuracy using methods
237 detailed in Supplementary Information.

238 *Statistics*

239 Effects of plant species, a[CO₂] and the interaction between these factors on the C,
240 ³³P and ¹⁵N fluxes between plants and Mucoromycotina fungi were tested using analysis of
241 variance (ANOVA) or Mann-Whitney U where indicated. Data were checked for homogeneity
242 and normality. Where assumptions for ANOVA were not met, data were transformed using
243 log₁₀. If assumptions for ANOVA were still not met, a Mann Whitney U statistical test was
244 performed. All statistics were carried out using the statistical software package SPSS
245 Version 24 (IBM Analytics, New York, USA). Stable isotope patterns were tested for
246 normality and equal variance. If the requirements of parametric data and equal variance
247 were fulfilled, one-way ANOVA was applied, while for non-parametric data Kruskal-Wallis
248 tests were performed. Leaves and roots were tested separately. Mean values are given with
249 standard deviations.

250

251 **Results**

252 *Molecular identification of fungal symbionts*

253 Analysis of experimental *L. inundata* plants grown under ambient and elevated
254 a[CO₂] confirmed that they were colonised by Mucoromycotina fungi. Glomeromycotina
255 sequences were not detected. Mucoromycotina OTUs were detected before and after the
256 experiments (Supplementary Figure S2); these same OTUs had previously been identified in
257 wild-collected lycophytes from diverse locations [10].

258 Diverse and shared Mucoromycotina fungi OTUs were detected in wild *L. inundata*,
259 liverworts and angiosperms growing adjacently in the same UK locations (Supplementary
260 Table S2, Fig. S2-8) in the following combinations: *L. inundata*, *F. foveolata*, *M. caerulea*
261 and *J. bulbosus* (Thursley Common, Surrey); *L. inundata*, *F. foveolata* and *J. bulbosus*
262 (Norfolk); *F. foveolata* and *H. lanatus* (Lynn Crafnant, Wales). Mucoromycotina OTUs were
263 also detected in *L. inundata* from Studland Heath, Dorset.

264

265 *Cytology of fungal colonisation in plants*

266 Trypan blue staining and SEM revealed two distinct fungal symbiont morphologies
267 consisting of either coarse hyphae (>3 μm diameter) and large vesicles (>20 μm diameter)
268 or fine branching hyphae (<2 μm diameter) with small swellings/vesicles (usually 5-10 but up
269 to 15 μm diameter) (Figures 2-3). Both morphologies were observed in the gametophyte of
270 the liverwort *F. foveolata* (Figures 2a, b, 3a; Supplementary Figure S10), in the roots of the
271 grasses *H. lanatus* (Figure 2f) and *M. caerulea* (Figure 2g, h), and the rush *J. bulbosus*
272 (Figure 3h, i). In the roots of wild and experimental plants of *L. inundata*, only fine hyphae
273 were detected (Figures 2c-e, 3f, g). As in the other plants analysed, these fine hyphae were
274 aseptate and formed both intercalary and terminal swellings/vesicles but, in contrast to the
275 grasses, never arbuscules (Supplementary Figure S10). Similar fungal morphology was also
276 observed in protocorm cells of newly developing sporophytes (Figure 3b, c) and in
277 gametophytes of *L. inundata* (Supplementary Figure S11). However, in these early
278 developmental stages, fungal colonization exhibits a distinct zonation: an outer intracellular
279 zone and a more central, strictly intercellular zone (Figure 3d, e; Supplementary Figure S11b,
280 c, g). In the intracellular zone, fungal colonization is the same as in the sporophyte roots and
281 consists of fine hyphae with intercalary and terminal swellings/vesicles (Figure 3b, c;
282 Supplementary Figure S11i). Unique to the gametophyte generation, in the outermost
283 cortical layers, the fungus also forms tightly wound coils (hyphae up to 2.5 μm in diameter)
284 with larger vesicles (15-20 μm) (Supplementary Figure S11d), as described before in
285 *Lycopodium clavatum* [36]. Both gametophyte and early developmental stages of the
286 sporophyte generation develop a conspicuous central system of large, mucilage-filled
287 intercellular spaces. In this region, the fungus becomes strictly intercellular (Figure 3d, e;
288 Supplementary, Figure S11g). The intercellular hyphae are initially fine and with small
289 swellings/vesicles (Figure 3d, Supplementary Figure S11e), as their intracellular
290 counterparts, but soon enlarge and eventually reach diameters in excess of 3 μm
291 (Supplementary Figure S11f), with no swellings/vesicles present at this stage. While no

292 morphological differences were detected between fungal root associates of the two
293 experimental *Lycopodiella* grown under contrasting a[CO₂], those grown under 800 ppm
294 a[CO₂] had more colonization (44 out of 56 root segments; 79%) than those grown under
295 440 ppm a[CO₂] (31 out of 58 root segments; 53%).

296 *Lycophyte-to-fungus C transfer*

297 Unlike in non-vascular plants, carbon allocation to fungal symbionts by *L. inundata*
298 were not significantly affected by a[CO₂]. However, there were trends in line with previous
299 findings in liverworts; *L. inundata* allocated ca. 2.8 times more photosynthate to
300 Mucoromycotina fungi under the simulated Paleozoic a[CO₂] of 800 ppm (Figure 4a)
301 compared with plants that were grown under ambient a[CO₂] of 440 ppm (Figure 4a; Mann-
302 Whitney U = 194, *P* = 0.864, *n* = 20). In terms of total C transferred from plants to
303 Mucoromycotina, a similar trend was observed (Figure 4b) with *L. inundata* transferring ca.
304 2.7 times more C to Mucoromycotina fungal partners at elevated a[CO₂] concentrations of
305 800 ppm compared to those maintained under a[CO₂] of 440 ppm (Figure 4b; Mann-Whitney
306 U = 197.5, *P* = 0.942, *n* = 20).

307 *Fungus-to-lycophyte ³³P and ¹⁵N transfer*

308 Mucoromycotina fungi transferred ³³P and ¹⁵N to their plant hosts (Figure 4c-f). There
309 were no significant differences in the amounts of either ³³P or ¹⁵N tracer acquired by
310 Mucoromycotina in *L. inundata* plant tissue when grown under elevated a[CO₂] of 800 ppm
311 compared to plants grown under a[CO₂] conditions of 440 ppm, either in terms of absolute
312 quantities (Figure 4c, ANOVA [*F*_{1, 23} = 0.009, *P* = 0.924, *n* = 12]; Figure 4e, ANOVA [*F*_{1, 22} =
313 0.126, *P* = 0.726, *n* = 12]) or when normalised to plant biomass (Figure 4d, ANOVA [*F*_{1, 23} =
314 0.085, *P* = 0.774, *n* = 12] and Figure 4f, ANOVA [*F*_{1, 22} = 0.770, *P* = 0.390, *n* = 12]).

315 *Natural abundance δ¹³C and δ¹⁵N stable isotope signatures of plants*

316 All leaf $\delta^{13}\text{C}$ values ranged between -26.2 and -30.1 ‰ and root $\delta^{13}\text{C}$ values between
317 -24.5 and -28.9 ‰, while leaf $\delta^{15}\text{N}$ values ranged from 3.3 to -10.0 ‰ and root $\delta^{15}\text{N}$ values
318 from 3.1 to -5.9 ‰ (Figure 5). Leaves of the three groups, *L. inundata* (n = 6), *J. bulbosus* (n
319 = 6) and reference plants (n = 17), were significantly different in $\delta^{13}\text{C}$ ($H(2) = 8.758$; $p =$
320 0.013) and $\delta^{15}\text{N}$ ($H(2) = 21.434$; $P < 0.001$, Figure 5a). *L. inundata* leaves were significantly
321 depleted in ^{13}C compared to *J. bulbosus* leaves ($Q = 2.644$, $P < 0.05$) and a significant
322 depletion of *L. inundata* leaves compared to reference plant leaves ($Q = 2.662$, $P < 0.05$,
323 Figure 5a). The *J. bulbosus* leaves were not significantly different from reference plants in
324 $\delta^{13}\text{C}$. No significant difference was discovered for $\delta^{15}\text{N}$ in *L. inundata* and *J. bulbosus* leaves
325 ($Q = 1.017$, $P > 0.05$), while leaves of both species were significantly enriched in ^{15}N
326 compared to the reference plants ($Q = 2.968$, $P < 0.05$; $Q = 4.205$, $P < 0.05$, Figure 5a). For
327 the roots, only $\delta^{15}\text{N}$ showed significant differences between the three groups under
328 comparison ($F(2) = 34.815$; $P < 0.001$, Figure 5b). The *L. inundata* and *J. bulbosus* roots
329 were not significantly distinguished in $\delta^{15}\text{N}$, however, roots of both species were significantly
330 enriched in ^{15}N compared to reference plant roots ($q = 10.109$, $p < 0.001$; $q = 8.515$, $p <$
331 0.001, Figure 5b).

332

333 Discussion

334 Our results show that the symbiosis between *L. inundata* and Mucoromycotina FRE is
335 nutritionally mutualistic, with the fungus gaining plant-fixed C and the plant gaining fungal-
336 acquired nutrients (Figure 4a-f). Cytological analyses of the fungus colonising the roots of *L.*
337 *inundata* revealed a characteristic morphology consisting of fine, aseptate branching hyphae
338 with terminal and intercalary swellings/vesicles. This morphology matches that described
339 previously in a range of angiosperms colonized by FRE [16, 19] and here in grasses, a rush
340 and a liverwort, all harbouring fungi identified molecularly as Mucoromycotina. Thus, our
341 results provide compelling evidence for Mucoromycotina FRE being shared by plants
342 occupying key nodes in the land plant phylogeny - from early liverworts and vascular

343 lycophytes to the later diverging angiosperms - and that this association represents a
344 nutritional mutualism as much in vascular as in non-vascular plants [5, 18].

345 Our findings raise novel and important questions regarding the evolution of
346 mycorrhizal associations and the nature of widespread Mucoromycotina FRE fungal
347 symbioses: what role did these fungi play during the greening of the Earth >500 Ma? How
348 have these associations persisted and why are they so widespread today? We can now
349 begin to address these questions with the demonstration that a vascular plant assimilates
350 significant amounts of Mucoromycotina FRE-acquired ¹⁵N tracer, suggesting a significant
351 role for Mucoromycotina FRE in vascular plant nitrogen uptake, facilitating their persistence
352 across nearly all land plant lineages.

353 *Costs and benefits of hosting Mucoromycotina fungi*

354 The amount of C transferred from *L. inundata* to Mucoromycotina symbionts was not
355 significantly affected by a[CO₂] (Figure 4a, b), with the fungi maintaining C assimilation
356 across the a[CO₂] treatments, despite colonisation being more abundant within the roots of
357 plants grown under the elevated a[CO₂]. Previous studies [5, 18] have demonstrated
358 Haplomitriopsida liverwort-Mucoromycotina FRE nutritional mutualisms were affected by
359 a[CO₂], with the fungi gaining more C from their host liverworts under elevated a[CO₂].
360 Although these experiments were carried out at higher a[CO₂] concentrations (1,500 ppm)
361 than the present study (800 ppm), both *Haplomitrium gibbsiae* and *Treubia lacunosa*
362 transferred approximately 56 and 189 times less photosynthate, respectively, to their fungi [5,
363 18] under elevated a[CO₂] compared to *L. inundata* (Supplementary Table S3). This trend is
364 consistent with previous observations in vascular plants with Glomeromycotina AM [8].
365 When compared to other vascular plant-Glomeromycotina fungal symbioses in similar
366 experimental systems [8], it is clear that the relative C “cost” of maintaining Mucoromycotina
367 fungal symbionts is at least on a par with, if not greater than, that of maintaining
368 Glomeromycotina fungi.

369 Lycophytes are a significant node in land plant phylogeny, widely considered as a
370 diversification point in the mid-Paleozoic (480-360 Ma) characterised by the evolution of
371 roots, leaves and associated vasculature [22]. The significant depletion of ^{13}C observed in
372 the leaves of *L. inundata* (Figure 5) is unlikely to be related to C gains from its
373 Mucoromycotina fungal symbiont [37]; rather it may indicate that *L. inundata* regulate their
374 stomata differently from *J. bulbosus* or the reference plants tested, as $\delta^{13}\text{C}$ in tissues of
375 terrestrial plants may be driven by the water use efficiency of the plant [38]. Alongside
376 increased capacity for C capture and fixation, it is likely that increasing structural complexity
377 in land plants across evolutionary time resulted in greater plant nutrient demand.

378 Glomeromycotina AM are associated with facilitation of plant P uptake and occur
379 commonly in soils with low P availability [39, 40]. We observed no difference in the amount
380 of fungal-acquired ^{33}P tracer that was transferred to *L. inundata* sporophytes when $a[\text{CO}_2]$
381 was changed (Figure 4c, d). Given that *L. inundata* can regulate and maintain CO_2
382 assimilation and thus C fixation through stomata and vasculature, it is possible that a lower
383 $a[\text{CO}_2]$ would affect transfer of plant-fixed C to symbiotic fungi less than it might do in
384 poikilohydric liverworts. The amount of ^{33}P transferred to *L. inundata* plants was much less
385 than has previously been recorded for Mucoromycotina-associated liverworts [18] or for
386 Glomeromycotina-associated ferns and angiosperms [8], despite the same amount of ^{33}P
387 being made available, suggesting that Mucoromycotina fungi may not play a critical role in
388 lycophyte P nutrition. Our results contrast with the view that FRE enhance plant P uptake, at
389 least in soils with very low P [19, 41], raising questions regarding the role of FRE in *L.*
390 *inundata* given that they represent a significant C outlay. Previous experiments with
391 Mucoromycotina-associated liverworts suggest there is a role for the fungus in plant N
392 nutrition [14, 18].

393 Nitrogen is an essential element for plants that is available in soils in plant-
394 inaccessible organic forms and as plant-accessible inorganic nitrate and ammonium [42].
395 Our results show that although there was no significant difference in the amount of ^{15}N

396 transferred from Mucoromycotina to *L. inundata* under elevated or ambient a[CO₂] (Figure
397 4e, f), up to 391 times more ¹⁵N was transferred to *L. inundata* than in Haplomitriopsida
398 liverworts in comparable experiments (Supplementary Table S3) [18]. We also show that *L.*
399 *inundata* and *J. bulbosus* were significantly ¹⁵N enriched in comparison to co-occurring
400 reference plants with different mycorrhizal partners (Figure 5). This further supports our
401 experimental finding that Mucoromycotina symbionts play a significant role in host plant N
402 nutrition.

403 Some AM fungi transfer N to their associated hosts [43]; however, the ecological
404 relevance of AM-facilitated N uptake is widely debated, in particular the amounts of N
405 transferred to hosts compared to the overall N requirements of the plant [44]. Different
406 mycorrhizal associations, i.e. ecto-, ericoid and arbuscular mycorrhizas, can influence plant
407 δ¹⁵N [45]. While this distinction in N isotope abundance between plants with different
408 mycorrhizas is almost or completely lost in conditions of higher N isotope availability [34], it
409 becomes significantly different under severe N limitation [46]. Exclusive plant-
410 Mucoromycotina FRE symbioses seem to be rare, having been reported before only in the
411 earliest-diverging Haplomitriopsida liverworts [6, 14], while all other plants, including other
412 lycophytes [10], that form associations with these fungi appear able to do so also with
413 Glomeromycotina, often simultaneously [14]. It is possible that the major input to
414 *Lycopodiella* N nutrition and minor contribution to P nutrition by Mucoromycotina FRE reflect
415 such a specialised relationship considering heathland habitats have very low plant-available
416 N. Nevertheless, our present data combined with previous demonstrations of N transfer in
417 liverwort-Mucoromycotina symbioses [14, 18] and emerging evidence that Mucoromycotina
418 FRE, but not Glomeromycotina, are able to transfer N to host liverworts from organic
419 sources (Field *et al.* unpublished), all point to an important role of Mucoromycotina FRE in
420 host plant N nutrition. Indeed, our cytological analyses show that, differently from
421 *Lycopodiella* roots where only fine endophytes were observed (Figure 2; Table 1), all other
422 co-occurring plants (*F. foveolata*, *J. bulbosus*, *M. caerulea*) were also colonised by coarse
423 endophytes with cytology typical of Glomeromycotina (Table 1). The finer functional details,

424 in terms of N and P transfer, of this partnership in other vascular plants from a broader range
425 of habitats remain to be established; the challenge here will be to separate the nutritional
426 contributions of Mucoromycotina FRE and Glomeromycotina to host plants that are co-
427 colonized by both fungi, as it seems to be the prevailing condition in vascular plants,
428 especially angiosperms.

429 *Mucoromycotina fine root endophytes*

430 Mucoromycotina fungi within Endogonales colonising the gametophytes of liverworts
431 (*F. foveolata*) and lycophytes (*L. inundata*), the sporophytic protocorms and roots of
432 lycophytes (*L. inundata*) and the roots of angiosperms (*J. bulbosus*, *M. caerulea*, *H. lanatus*),
433 all display the same characteristic morphology attributed previously to FRE [16, 19]. This
434 contrasts with that typical of Glomeromycotina fungal associations, consisting of coarse
435 hyphae (>3 µm diameter) and larger vesicles, which we observed in *Fossombronina*, *Juncus*,
436 *Molinia*, *Holcus* but not in *L. inundata* (Table 1). These observations together with molecular
437 identification of Mucoromycotina clades shared by these phylogenetically distant plant
438 lineages support previous suggestions that vascular plants' FRE are closely related to the
439 Mucoromycotina mycorrhizal-like symbionts of non-vascular plants [15]. Here, we show that
440 the same Mucoromycotina FRE are symbiotic across different land plant phyla.

441 Our demonstration of an extensive intercellular phase of fungal colonisation in the
442 gametophytes and protocorms of *L. inundata* is in line with other lycophytes [10, 36] and
443 strongly recalls the gametophytes of the Haplomitriopsida liverwort *Treubia* [31] and several
444 hornworts [9], all of which have also been shown to associate with Mucoromycotina fungi [6,
445 9]. Differently from their fine intracellular counterparts, intercellular hyphae become swollen,
446 eventually reaching more than 3 µm in diameter. Tightly wound hyphal coils up to 2.5 µm in
447 diameter with somewhat larger terminal vesicles (up to 20 µm in diameter) are also
448 prominent in the outer cortical layers of *L. inundata* gametophytes but were not observed in
449 either protocorms or roots. Thus, Mucoromycotina FRE display considerable phenotypic

450 plasticity in their interactions with ancient lineages of land plants which appears to relate to
451 the developmental stage of the host and whether it produces an extensive network of
452 mucilage-filled intercellular spaces. Comparable intercellular proliferation patterns alongside
453 intracellular fungal structures have been described in the Devonian fossil plant
454 *Horneophyton ligneri* and attributed to Mucoromycotina [7], closely resembling the distinctive
455 inter- and extracellular fungal colonisation of another Devonian fossil plant, *Nothia* [47]
456 (Table 1). The putative occurrence of Mucoromycotina FRE in early land plants and their
457 presence in both extant early and later diverging plant lineages now point to a prominent role
458 of these fungi, not only in plant terrestrialization [14], but also in current ecosystem
459 functioning. Indeed, Mucoromycotina FRE have been shown to occur worldwide across
460 many ecosystems, particularly in the roots of crop and pasture species, where colonization
461 levels may be high, even as dense as the biomass of coarse Glomeromycotina arbuscular
462 mycorrhizal fungi [19].

463

464 *More ammunition for the mycorrhizal revolution*

465 Our findings provide, for the first time, conclusive evidence that Mucoromycotina
466 FRE form nutritional mutualisms not only with non-vascular liverworts [5, 18] but also with a
467 vascular plant. In line with previous reports showing nutritional mutualisms between non-
468 vascular plants and Mucoromycotina fungi, with the exception of *Treubia lacunosa* [5, 8, 18],
469 our experimental system was not significantly affected by a[CO₂] concentrations. However,
470 we report that *L. inundata* transfers up to 189 times more photosynthate to Mucoromycotina
471 fungi than a non-vascular plant [5, 18]. In addition, we found that Mucoromycotina fungi
472 transfer less ³³P tracer, but can transfer ca. 391 times more ¹⁵N tracer to a vascular than to a
473 non-vascular plant [18]. In contrast, the literature on FRE so far has focused on P [19]. From
474 an evolutionary standpoint, our findings point towards a new physiological niche for the
475 persistence of Mucoromycotina fungi from ancient to modern plants, both singly and in dual

476 colonisation with Glomeromycotina.

477 **Acknowledgements**

478 We gratefully acknowledge support from the NERC to KJF, SP, SS (NE/N00941X/1) and
479 MIB (NE/N009665/1). KJF is funded by BBSRC Translational Fellowship (BB/M026825/1).
480 WRR is supported by a NERC DTP (Science and Solutions for a Changing Planet)
481 studentship. We thank James Giles (Natural England) for field support, Julia Masson and the
482 RSPB for access to the Norfolk site, and The Species Recovery Trust for access to the
483 Dorset site.

484 **References**

- 485 1. Morris JL, Puttick MN, Clark JW, Edwards D, Kenrick P, Pressel S *et al.* The timescale
486 of early land plant evolution. *Proc. Natl. Acad. Sci.* 2018; **115**(10): 2274-2283.
- 487 2. Berner RA. GEOCARBSULF: a combined model for Phanerozoic atmospheric O₂ and
488 CO₂. *Geochim. Cosmochim. Acta.* 2006; **70**(23): 5653-5664.
- 489 3. Pirozynski KA, Malloch DW. The origin of land plants: A matter of mycotrophism.
490 *Biosyst.* 1975; **6**(3): 153-164.
- 491 4. Redecker D, Kodner R, Graham LE. Glomalean fungi from the Ordovician. *Science.*
492 2000; **289**(5486): 1920-1921.
- 493 5. Field KJ, Rimington WR, Bidartondo MI, Allinson KE, Beerling DJ, Cameron DD *et al.*
494 First evidence of mutualism between ancient plant lineages (Haplomitriopsida
495 liverworts) and Mucoromycotina fungi and its response to simulated Palaeozoic
496 changes in atmospheric CO₂. *New Phytol.* 2015; **205**(2): 743-756.
- 497 6. Bidartondo MI, Read DJ, Trappe JM, Merckx V, Ligrone R, Duckett JG. The dawn of
498 symbiosis between plants and fungi. *Biol. Lett.* 2011; **7**: 574-577.

- 499 7. Strullu - Derrien C, Kenrick P, Pressel S, Duckett JG, Rioult JP, Strullu DG. Fungal
500 associations in Horneophyton ligneri from the Rhynie Chert (c. 407 million year old)
501 closely resemble those in extant lower land plants: novel insights into ancestral
502 plant–fungus symbioses. *New Phytol.* 2014; **203**(3): 964-979.
- 503 8. Field KJ, Cameron DD, Leake JR, Tille S, Bidartondo MI, Beerling DJ. Contrasting
504 arbuscular mycorrhizal responses of vascular and non-vascular plants to a simulated
505 Palaeozoic CO₂ decline. *Nat. Comms.* 2012; **3**: 835.
- 506 9. Desirò A, Duckett JG, Pressel S, Villareal JC, Bidartondo MI. Fungal symbioses in
507 hornworts: a chequered history. *Proc. Roy. Soc. Lond. B.* 2013; **280**(1759): 20130207.
- 508 10. Rimington WR, Pressel S, Duckett JG, Bidartondo MI. Fungal associations of basal
509 vascular plants: reopening a closed book? *New Phytol.* 2015; **205**(4): 1394-1398.
- 510 11. James TY, Kauff F, Schoch CL, Matheny PB, Hofstetter V, Cox CJ, *et al.* Reconstructing
511 the early evolution of Fungi using a six-gene phylogeny. *Nature.* 2006; **443**(7113):
512 818-822.
- 513 12. Lin K, Limpens E, Zhang Z, Ivanov S, Saunders DG, Mu D, *et al.* Single nucleus genome
514 sequencing reveals high similarity among nuclei of an endomycorrhizal fungus. *PLoS*
515 *Genet.* 2014; **10**(1): e1004078.
- 516 13. Krings M, Taylor TN, Hass H, Kerp H, Dotzler N, Hermsen EJ. An alternative mode of
517 early land plant colonization by putative endomycorrhizal fungi. *Plant Signal. Behav.*
518 2007; **2**(2): p. 125-126.
- 519 14. Field KJ, Pressel S, Duckett JG, Rimington WR, Bidartondo MI. Symbiotic options for
520 the conquest of land. *Trends Ecol. Evol.* 2015; **30**(8): 477-486.

- 521 15. Rimington WR, Pressel S, Field KJ, Strullu-Derrien C, Duckett JG, Bidartondo MI.
522 Reappraising the origin of mycorrhizas. In: Martin F (ed). *Molecular Mycorrhizal*
523 *Symbiosis*, Wiley Blackwell Publishing Ltd: USA, 2016, pp 31-32.
- 524 16. Orchard S, Hilton S, Bending GD, Dickie IA, Standish RJ, Gleeson DB, *et al.* Fine
525 endophytes (*Glomus tenue*) are related to Mucoromycotina, not Glomeromycota.
526 *New Phytol.* 2017; **213**(2): 481-486.
- 527 17. Hoysted GA, Kowal J, Jacob A, Rimington WR, Duckett JG, Pressel S, *et al.* A
528 mycorrhizal revolution. *Curr. Opin. Plant Biol.* 2018; **44**: 1-6.
- 529 18. Field KJ, Rimington WR, Bidartondo MI, Allinson KE, Beerling DJ, Cameron DD, *et al.*
530 Functional analysis of liverworts in dual symbiosis with Glomeromycota and
531 Mucoromycotina fungi under a simulated Palaeozoic CO₂ decline. *ISME J.* 2016;
532 **10**(6): 1514-1526.
- 533 19. Orchard S, Standish RJ, Dickie IA, Renton M, Walker C, Moot D, *et al.* Fine root
534 endophytes under scrutiny: a review of the literature on arbuscule-producing fungi
535 recently suggested to belong to the Mucoromycotina. *Mycorrhiza.* 2017; **27**(7): 619-
536 638.
- 537 20. Walker C, Gollotte A, Redecker D. A new genus, *Planticonsortium* (Mucoromycotina),
538 and new combination (*P. tenue*), for the fine root endophyte, *Glomus tenue*
539 (basionym *Rhizophagus tenuis*). *Mycorrhiza*, 2018; **28**(3): 1-7.
- 540 21. Field KJ, Pressel S. Unity in diversity: structural and functional insights into the
541 ancient partnerships between plants and fungi. *New Phytol.* 2018.
- 542 22. Kenrick P, Crane PR. The origin and early evolution of plants on land. *Nature.* 1997;
543 **389**(6646): 33-39.

- 544 23. Duckett JG, Ligrone, R. A light and electron microscope study of the fungal
545 endophytes in the sporophyte and gametophyte of *Lycopodium cernuum* with
546 observations on the gametophyte–sporophyte junction. *Can. J. Bot.* 1992; **70**(1): 58-
547 72.
- 548 24. Brundrett M, Bougher N, Dell B, Grove T. Working with mycorrhizas in forestry and
549 agriculture. 1996.
- 550 25. Kearse M, Moir R, Wilson A, Stones-Havas S, Cheung M, Sturrock S, *et al.* Geneious
551 Basic: an integrated and extendable desktop software platform for the organization
552 and analysis of sequence data. *Bioinformatics.* 2012; **28**(12): 1647-1649.
- 553 26. Edgar R. UCHIME2: improved chimera prediction for amplicon sequencing. *BioRxiv.*
554 2016; 074252.
- 555 27. Kumar S, Stecher G, Tamura K. MEGA7: molecular evolutionary genetics analysis
556 version 7.0 for bigger datasets. *Mol. Biol. Evol.* 2016; **33**(7): 1870-1874.
- 557 28. Guindon S, Gascuel O. A simple, fast, and accurate algorithm to estimate large
558 phylogenies by maximum likelihood. *Syst Biol.* 2003; **52**(5): 696-704.
- 559 29. Ronquist F, Huelsenbeck JP. MrBayes 3: Bayesian phylogenetic inference under
560 mixed models. *Bioinformatics.* 2003; **19**(12): 1572-1574.
- 561 30. Orchard S, Standish RJ, Nicol D, Dickie IA, Ryan MH. Sample storage conditions alter
562 colonisation structures of arbuscular mycorrhizal fungi and, particularly, fine root
563 endophyte. *Plant Soil.* 2017; **412**(1-2): 35-42.
- 564 31. Duckett JG, Carafa A, Ligrone R. A highly differentiated glomeromycotean association
565 with the mucilage-secreting, primitive antipodean liverwort *Treubia* (Treubiaceae):
566 clues to the origins of mycorrhizas. *Am. J. Bot.* 2006; **93**(6): 797-813.

- 567 32. Cameron DD, Johnson I, Leake JR, Read DJ. Mycorrhizal acquisition of inorganic
568 phosphorus by the green-leaved terrestrial orchid *Goodyera repens*. *Ann. Bot.* 2007;
569 **99**(5): 831-834.
- 570 33. Cameron DD, Leake JR, Read DJ. Mutualistic mycorrhiza in orchids: evidence from
571 plant–fungus carbon and nitrogen transfers in the green - leaved terrestrial orchid
572 *Goodyera repens*. *New Phytol.* 2006; **171**(2): 405-416.
- 573 34. Gebauer G, Meyer M. ¹⁵N and ¹³C natural abundance of autotrophic and myco -
574 heterotrophic orchids provides insight into nitrogen and carbon gain from fungal
575 association. *New Phytol.* 2003; **160**(1): 209-223.
- 576 35. Bidartondo MI, Burghardt B, Gebauer G, Bruns TD, Read DJ. Changing partners in the
577 dark: isotopic and molecular evidence of ectomycorrhizal liaisons between forest
578 orchids and trees. *Proc. Roy. Soc. Lond. B.* 2004; **271**(1550): 1799-1806.
- 579 36. Schmid E, Oberwinkler F. Mycorrhiza - like interaction between the achlorophyllous
580 gametophyte of *Lycopodium clavatum* L. and its fungal endophyte studied by light
581 and electron microscopy. *New Phytol.* 1993; **124**(1): 69-81.
- 582 37. Bago B, Pfeffer PE, Shachar-Hill Y. Carbon metabolism and transport in arbuscular
583 mycorrhizas. *Plant Physiol.* 2000; **124**(3): 949-958.
- 584 38. Farquhar GD, Ehleringer JR, Hubick, KT. Carbon isotope discrimination and
585 photosynthesis. *Ann. Rev. Plant Biol.* 1989; **40**(1): 503-537.
- 586 39. Smith SE, Anderson IC, Smith FA. Mycorrhizal associations and phosphorus
587 acquisition: from cells to ecosystems. *Ann. Plant. Rev.* 2015; **48**: 409-440.
- 588 40. Albornoz FE, Lambers H, Turner BL, Teste FP, Laliberté E. Shifts in symbiotic
589 associations in plants capable of forming multiple root symbioses across a long -
590 term soil chronosequence. *Ecol. Evol.* 2016; **6**(8): 2368-2377.

- 591 41. Ryan MH, Kirkegaard JA. The agronomic relevance of arbuscular mycorrhizas in the
592 fertility of Australian extensive cropping systems. *Agric. Ecosyst. Environ.* 2012; **163**:
593 37-53.
- 594 42. Krapp A. Plant nitrogen assimilation and its regulation: a complex puzzle with missing
595 pieces. *Curr. Opin. Plant Biol.* 2015; **25**: 115-122.
- 596 43. Hodge A, Campbell CD, Fitter AH. An arbuscular mycorrhizal fungus accelerates
597 decomposition and acquires nitrogen directly from organic material. *Nature.* 2001;
598 **413**(6853): 297-299.
- 599 44. Smith SE, Smith FA. Roles of arbuscular mycorrhizas in plant nutrition and growth:
600 new paradigms from cellular to ecosystem scales. *Annu. Rev. Plant Biol.* 2011; **62**:
601 227-250.
- 602 45. Dawson TE, Mambelli S, Plamboeck AH, Templer PH, Tu KP. Stable isotopes in plant
603 ecology. *Ann. Rev. Ecol. Syst.* 2002; **33**(1): 507-559.
- 604 46. Schulze ED, Chapin FS, Gebauer G. Nitrogen nutrition and isotope differences among
605 life forms at the northern treeline of Alaska. *Oecol.* 1994; **100**(4): 406-412.
- 606 47. Krings M, Taylor TN, Hass H, Kerp H, Dotzler N, Hermsen EJ. Fungal endophytes in a
607 400 - million - yr - old land plant: infection pathways, spatial distribution, and host
608 responses. *New Phytol.* 2007; **174**(3): 648-657.

609

610

611

612 **Figure legends**

613

614 **Figure 1. Land plant phylogeny and species used in the present study.** (a) Land plant
615 phylogeny showing key nodes alongside commonly associated fungal symbionts [6, 11, 23,
616 31] (b) *Lycopodiella inundata* at Thursley Common, Surrey, June 2017.

617

618 **Figure 2. Light micrographs of trypan blue stained tissues.** (a) Branching fine hyphae
619 with small swellings/vesicles in thallus cells and rhizoid (b) of the liverwort *Fossombronia*
620 *foveolata* colonized by both Mucoromycotina fine root endophytes (FRE) and
621 Glomeromycotina, in (b) also note the coarse hyphae (arrowhead). (c-e) Fine hyphae with
622 small swellings/vesicles in the root hairs and root cells of the lycophyte *Lycopodiella*
623 *inundata* colonized by Mucoromycotina FRE only. (f) Fine hyphae with small
624 swellings/vesicles and large vesicles in a root of the grass *Holcus lanatus* colonized by both
625 Mucoromycotina FRE and Glomeromycotina. (g-h) Roots of the grass *Molinia caerulea*
626 colonized by both Mucoromycotina FRE and Glomeromycotina, showing fine hyphae (g) and
627 coarse hyphae with large vesicles (h). Scale bars: (a, b, d-f) 50 μm , (c, g, h) 100 μm .

628 **Figure 3. Scanning electron micrographs.** (a) Fine hyphae (arrows) with a small
629 swelling/vesicle (*) in the thallus cells of *Fossombronia foveolata*, also note the much
630 coarser hyphae (arrowheads). (b-g) Fungal colonization in *Lycopodiella inundata*. (b, c)
631 Intercalary (b) and terminal (c) small swellings/vesicles on fine hyphae in the ventral cell
632 layers of a protocorm. Centrally and above this intracellular colonization zone, the fungus
633 becomes exclusively intercellular (d, e). (f, g) Cross sections of roots showing branching fine
634 hyphae with small swellings/vesicles. (h, i) Cross sections of roots of *Juncus bulbosus*
635 showing fine (arrow) and coarse (arrowheads) hyphae (h) and a fine hypha with small
636 swellings/vesicles (i). Scale bars: (e) 500 μm , (f) 50 μm , (a, d, g, i) 20 μm , (b, c, h) 10 μm .

637

638 **Figure 4. Carbon-for-nutrient exchange between *Lycopodiella inundata* and**
639 **Mucoromycotina fine root endophyte fungi.** (a) % allocation of plant-fixed C to
640 Mucoromycotina fungi (b) Total plant-fixed C transferred to Mucoromycotina fungi by *L.*
641 *inundata*. (c) Total plant tissue ^{33}P content (ng) and (d) tissue concentration (ng g^{-1}) of
642 fungal-acquired ^{33}P in *L. inundata* tissue (e) Total tissue ^{15}N content (ng) and (f)
643 concentration (ng g^{-1}) of fungal-acquired ^{15}N in *L. inundata* with exclusive Mucoromycotina
644 fungal associations. All experiments conducted at a[CO₂] of 800 p.p.m. (black bars) and 440

645 p.p.m. (white bars). All bars in each panel represent the difference in isotopes between the
646 static and rotated cores inserted into each microcosm. In all panels, error bars denote SEM.
647 In panels a and b $n = 20$ for both a[CO₂]. In panels c-f $n = 12$ for both 800 p.p.m and 440
648 p.p.m a[CO₂].

649

650 **Figure 5. Carbon and nitrogen stable isotope natural abundance of *Lycopodiella***
651 ***inundata* and surrounding angiosperms. (a)** Data from leaves. **(b)** Data from roots.

652

653 **Table 1. Cytology of colonisation and fungal identity of study species (*) compared to**
654 **relevant examples from the literature** (referred to in Discussion).

655 *Results from this study; G = gametophyte generation; S = sporophyte generation; ICSs =
656 intercellular spaces

657

658 **Author's contributions**

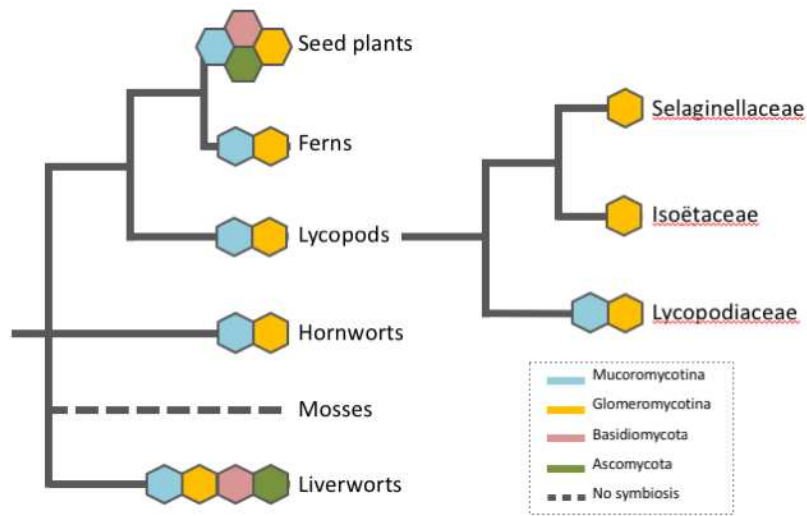
659 K.J.F., S.P., S.S., M.I.B., and J.G.D. conceived and designed the investigation. S.P., J.K.,
660 J.G.D., M.I.B., A.S.J. and G.A.H collected plant material. G.A.H. and K.J.F. undertook the
661 physiological analyses. A.S.J., W.R.R. and M.I.B. undertook the molecular analyses. S.P.
662 undertook the cytological analyses with assistance from J.K. P.G. and G.G. analysed and
663 interpreted the stable isotope data. All authors discussed results and commented on the
664 manuscript.

665 **Competing interests statement**

666 There are no conflicts of interest.

667

A



B



Fig. 1

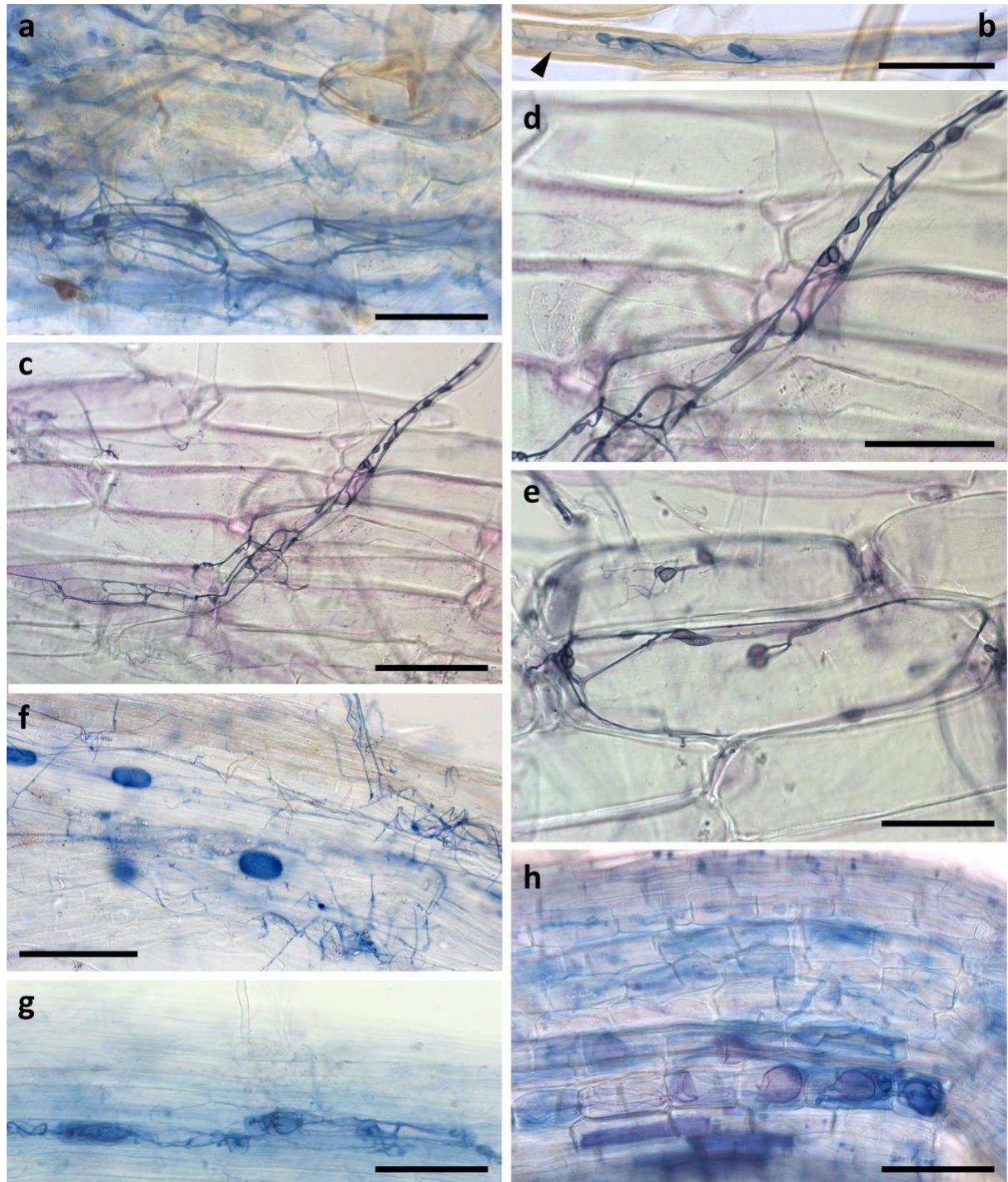


Fig. 2

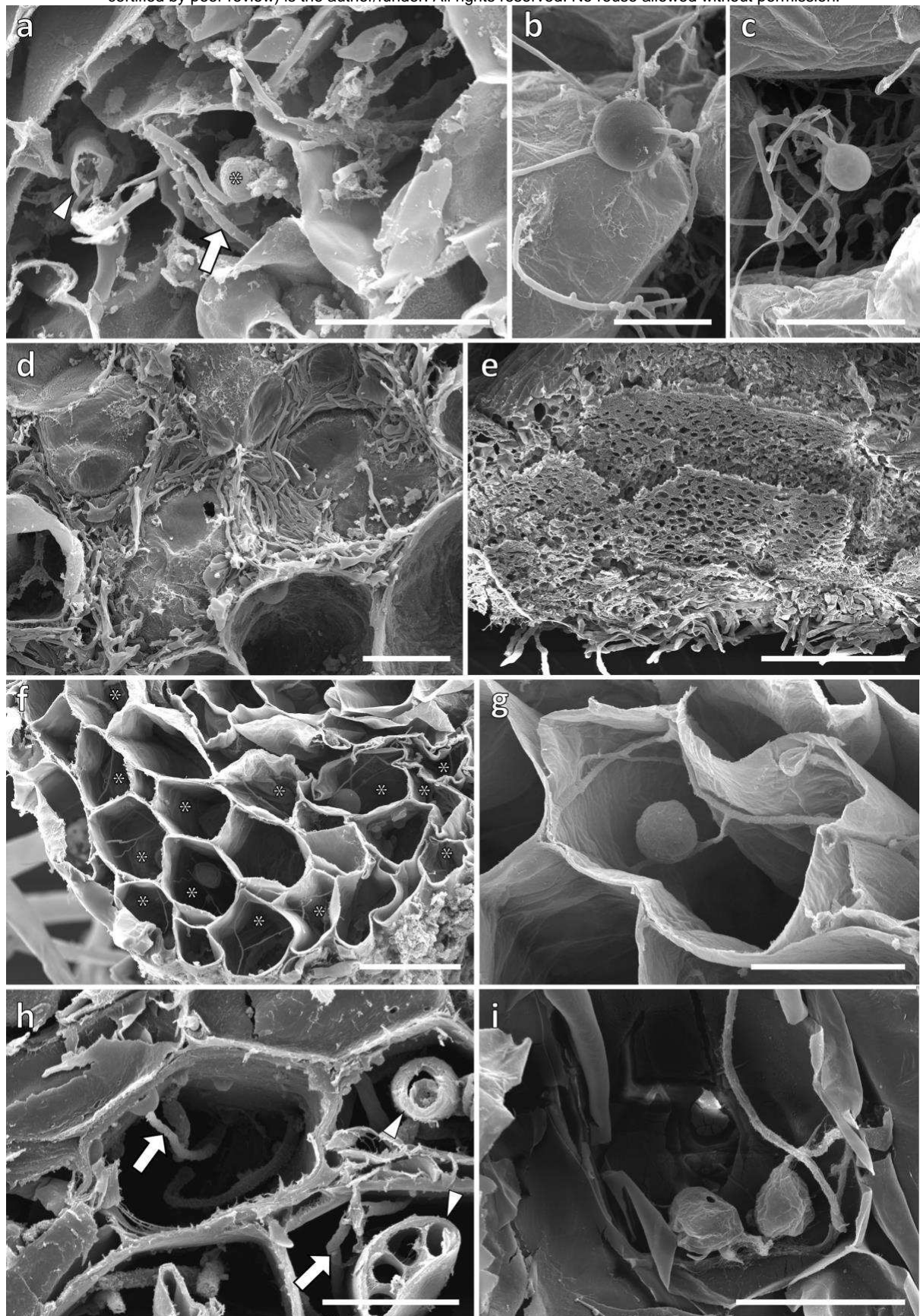


Figure 3.

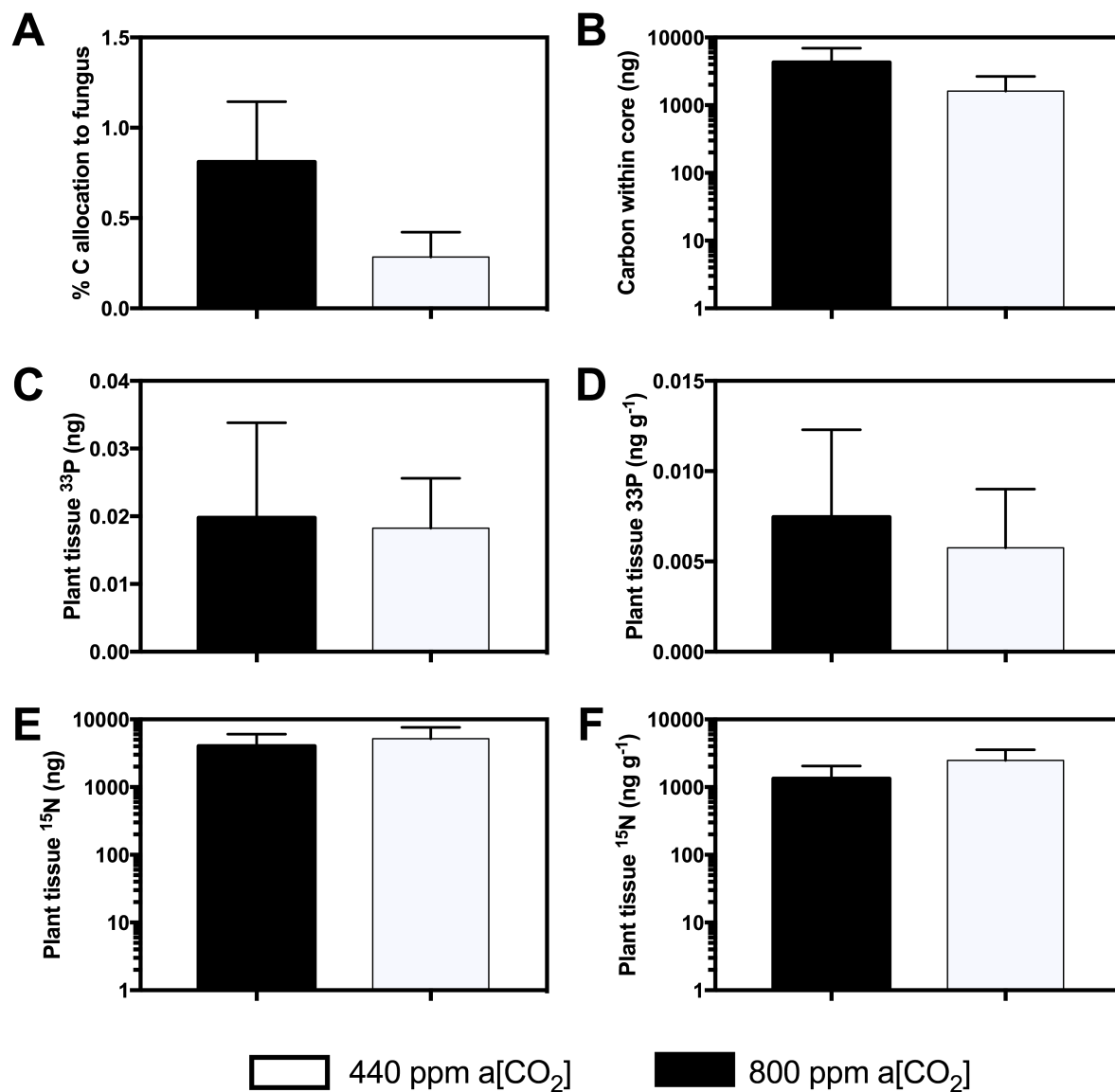


Figure 4.

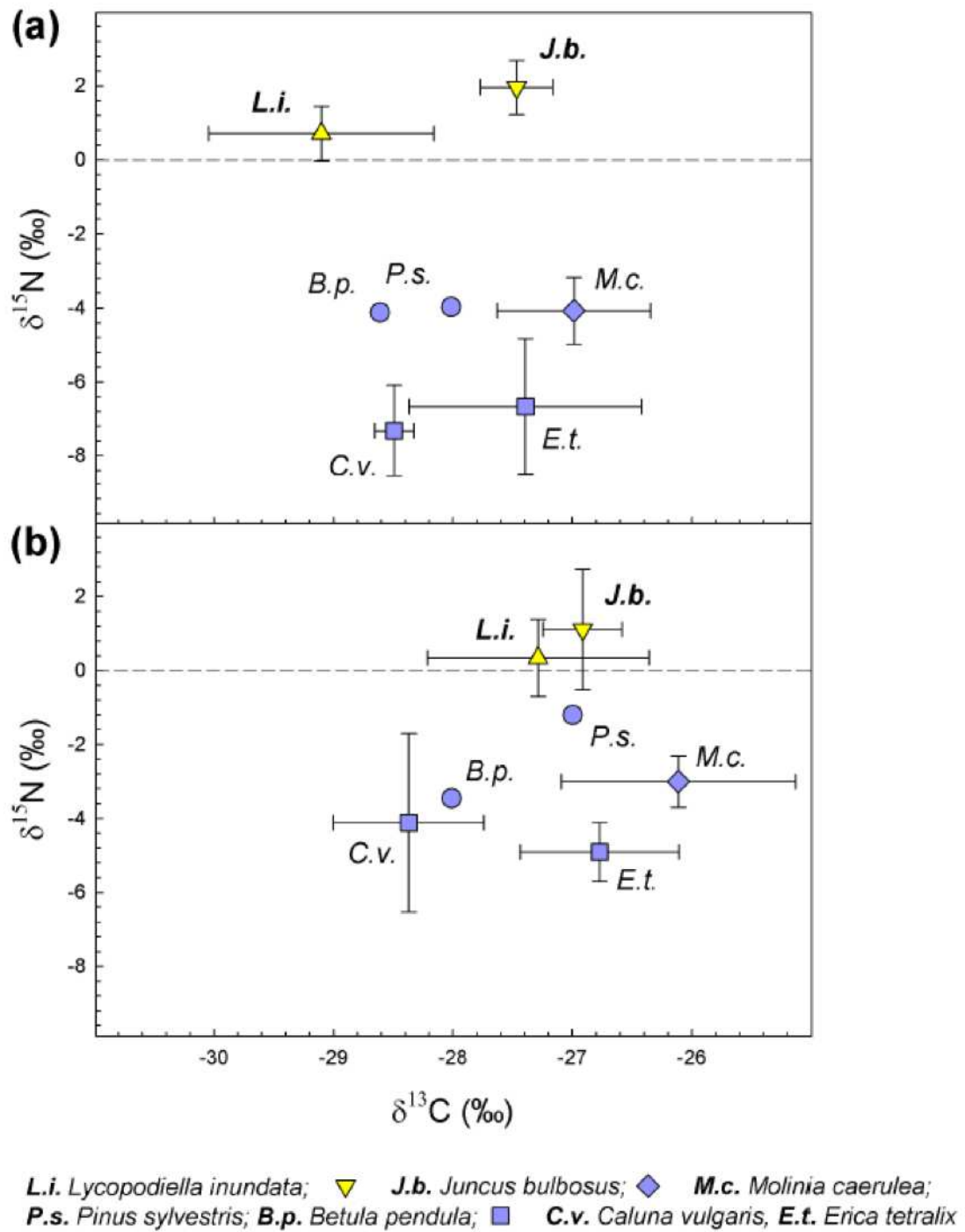


Figure 5.

1 **Table 1. Cytology of colonisation and fungal identity of study species (*) compared to**

2 **relevant examples from the literature that are referred to in the Discussion.**

3 *Results from this study; G = gametophyte generation; S = sporophyte generation; ICSS =

4 intercellular spaces

5

	G/ S	Tissue/location	Colonization	Morphology (diameter)	Fungus ID	References
Liverworts						
<i>Treubia</i> ¹	G	several ventral cell layers	intracellular	coils (0.5-1.5 µm) with 'lumps'/swellings (up to 15 µm), arbuscule-like short-side branches on coiled hyphae	M ²	⁴³ Duckett <i>et al.</i> 2006 ⁵ Bidartondo <i>et al.</i> 2011
		above intracellular zone	intercellular: large mucilage-filled ICSSs	coarse hyphae 2-3 µm, thick-walled fungal structures		
<i>Fossombronia</i> *	G	thallus central strand	intracellular	coarse hyphae (2-3 µm); large vesicles (15-30 µm), coils (0.5-1 µm), fine hyphae (0.5-1.5 µm) with small swellings/vesicles (5-10 µm), arbuscules	(M&G)*	
Lycophytes						
<i>Lycopodiella</i> *	G	outer cortical cell layers	intracellular	coils (up to 2.5µm) with vesicles (15-20µm), fine hyphae (0.5-1.5 µm) with small swellings/vesicles (5-10 µm)	M*	
		several ventral cell layers	intracellular			
		above intracellular zone	intercellular: large mucilage-filled ICSSs	coarse hyphae (2- >3 µm)		
	S	protocorm: several ventral cell layers central, above intracellular zone	intracellular intercellular: large mucilage-filled ICSSs	fine hyphae (0.5-1.5 µm) with small swellings/vesicles (5-10 µm) coarse hyphae (2- >3 µm)	M*	
	S	root	intracellular and intercellular, small ICSSs	fine hyphae (0.5-1.5 µm) with small swellings/vesicles (5-15 µm)	M ¹ *	⁹ Rimington <i>et al.</i> 2015
Angiosperms						
<i>Holcus</i> *	S	root	intracellular and intercellular, small ICSSs	coarse hyphae (>3 µm), large vesicles (20-40 µm), fine hyphae (0.5-1.5 µm) with small vesicles (5-10 µm), arbuscules/arbuscule-like structures	(M&G)*	
<i>Molinia</i> *	S	root	intracellular and intercellular, small ICSSs	coarse hyphae (>3 µm), large vesicles (20-40 µm), fine hyphae (0.5-1.5 µm) with small vesicles/swellings (5-10 µm), arbuscules/arbuscule-like structures	(M&G)*	
<i>Juncus</i> *	S	root	intracellular and intercellular, small ICSSs	coarse hyphae (>3 µm), large vesicles (20-40 µm), fine hyphae (0.5-1.5 µm) with small vesicles (5-10 µm), arbuscules/arbuscule-like structures	(M&G)*	

<i>Trifolium</i> ¹	S	root	intracellular and intercellular, small ICSs	coarse hyphae (>3 μm), large vesicles (>30 μm) fine hyphae (>1.5 μm), intercalary and terminal vesicles/swellings (5-10 μm) and arbuscules/arbuscule-like structures	(M&G) ¹	¹⁵ Orchard <i>et al.</i> 2017
Fossils						
<i>Horneophyton</i> ¹	S	aerial axes, cortical cells	intracellular	coarse hyphae (>3 μm), large vesicles (up to 50 μm), arbuscule-like structures	G ¹	⁶ Strullu-Derrien <i>et al.</i> 2014
		corm	intracellular and intercellular	intracellular coils, intercellular coarse hyphae (11-13 μm), thick-walled fungal structures	M ¹	
<i>Nothia</i> ¹	S	aerial and prostrate axes	intercellular and intracellular	coarse hyphae (up to 15 μm) and intercellular vesicles (>50 μm)	?	¹² Krings <i>et al.</i> 2007

6

7